

Polarised electromagnetic wave propagation through the ferromagnet: Phase boundary of dynamic phase transition

Muktish Acharyya

*Department of Physics, Presidency University,
86/1 College Street, Calcutta-700073, India
E-mail:muktish.physics@presiuniv.ac.in*

Abstract: The dynamical responses of ferromagnet to the propagating electromagnetic field wave passing through it are modelled and studied here by Monte Carlo simulation in two dimensional Ising model. Here, the electromagnetic wave is linearly polarised in such a way that the direction of magnetic field is parallel to that of the magnetic spins. The coherent spin-cluster propagating mode is observed. The time average magnetisation over the full cycle (time) of the field defines the order parameter of the dynamic phase transition. Depending on the value of the temperature and the amplitude of the propagating magnetic field wave, a dynamical phase transition is observed. The transition is detected by studying the temperature dependences of the variance of the dynamic order parameter, the derivative of the dynamic order parameter and the dynamic specific heat. The phase boundary of the dynamic transitions are drawn for two different values of the wave length of the propagating magnetic field wave. The phase boundary is observed to shrink (inward) for shorter wavelength of the EM wave. The signature of the divergence of the relevant length scale is observed at the transition point.

PACS Nos:05.50.+q, 05.70.Ln, 75.30.Ds, 75.30.Kz, 75.40.Gb

Keywords: Ising ferromagnet, Monte Carlo simulation, Polarised electromagnetic wave, Dynamic phase transition

I. Introduction.

The dynamical response of Ising ferromagnet to a time dependent magnetic field has become an active field of research [1]. The hysteretic responses and the nonequilibrium dynamic phase transitions are two main points of attention. The scaling behaviour [2] of hysteresis loop area with the amplitude, frequency of the sinusoidally oscillating magnetic field is the main outcome of the research. Another interesting aspect is the nonequilibrium dynamic phase transition which has produced variety of interesting results and prompted the researchers to take continuous attention in this field. Historically, some important observations like (i) divergences of dynamic specific heat and relaxation time near the transition point [3], (ii) divergence of the relevant length-scale near the transition point [4], (iii) studies regarding the existence of tricritical point [5, 6], (iv) the relation with the stochastic resonance [5] and the hysteretic loss [7], enriched the field and established that the dynamic transition has similarity to the well-known equilibrium thermodynamic phase transition. Very recently, a surface dynamic phase transition [8] is observed in kinetic Ising ferromagnet driven by oscillating magnetic field. The dynamic phase transition was detected also experimentally [9] in ultrathin Co film on Cu(001) system by surface magneto-optic Kerr effect. The direct excitation of propagating spin waves by focused ultrashort optical pulses are investigated recently [10]. The transient behaviour of the dynamically ordered phase in uniaxial Cobalt film is also studied experimentally [11].

This dynamic phase transition is also observed in other magnetic models. The off-axial dynamic phase transition was observed [12] in the anisotropic classical Heisenberg model and in the XY model [13]. The multiple (surface and bulk) dynamic transition was observed [14] in the classical Heisenberg model. The multiple dynamic transition was found [15] also in the Heisenberg ferromagnet driven by polarised magnetic field. The dynamic transition was observed [16] in the kinetic spin-3/2 Blume-Capel model and in the Blume-Emery-Griffith model [17] by meanfield calculations. The dynamic phase transition was studied by Monte Carlo simulation [18] and by meanfield calculation [19] in Ising metamagnet.

It may be noted here, that all the studies mentioned so far, were done by sinusoidally oscillating magnetic field which was uniform over the space (lattice) at any instant of time. In those studies, the spatio-temporal variation of applied magnetic field was not considered. One such spatio-temporal

variation of applied magnetic field would be the propagating magnetic field wave. In reality, if the electromagnetic wave passes through the ferromagnet, the varying (with space and time) magnetic field coupled with the spin, will affect the dynamic nature of the system. Here also dynamic transition will be observed. Very recently, it is reported briefly [20] that propagating magnetic field wave would lead to dynamical phase transition in Ising ferromagnet. A pinned phase and a phase of coherent motion of spin-clusters were observed recently [21] in random field Ising model, swept by propagating magnetic field wave. Here the nonequilibrium dynamic phase transition is *athermal* and tuned by quenched random (field) disorder. A rich dynamical phase boundary (with four different phases) was also drawn. A dynamic symmetry breaking breathing and spreading transitions [22] are also found recently in ferromagnetic film irradiated by spherical electromagnetic wave.

Here, in this paper, the nonequilibrium dynamic phase transition is studied extensively in two dimensional Ising ferromagnet swept by polarised propagating electromagnetic field wave. The technique employed here is Monte Carlo (MC) simulation. The phase boundary of the dynamical phase transition is drawn in this study. The paper is organised as follows: The model and the MC simulation technique are discussed in section-II, the numerical results are reported in section-III and the paper ends with a summary, in section-IV.

II. Model and Simulation.

The Hamiltonian (time dependent) representing the two dimensional Ising ferromagnet (having uniform nearest neighbour interaction) in presence of a polarised propagating electromagnetic field wave (having spatio-temporal variation) can be written as,

$$H(t) = -J\sum s(x, y, t)s(x', y', t) - \sum h(x, y, t)s(x, y, t). \quad (1)$$

The $s(x, y, t)$ represents the Ising spin variable (± 1) at lattice site (x, y) at time t on a square lattice of linear size L . $J(> 0)$ is the ferromagnetic (taken here as uniform) interaction strength. The summation in the first term represents the Ising spin-spin interaction and is carried over the nearest neighbours only. The $h(x, y, t)$ is the value of the magnetic field (at point (x, y) and at any time t) of the propagating electromagnetic wave. It may be noted here that the electromagnetic wave is linearly polarised in such a

way that the direction of magnetic field is parallel to that of the spins. For a propagating magnetic field wave $h(x, y, t)$ takes the form

$$h(x, y, t) = h_0 \cos(2\pi ft - 2\pi y/\lambda) \quad (2)$$

The h_0 , f and λ represent the amplitude, frequency and the wavelength respectively of the propagating electromagnetic field wave which propagates along the y -direction. In the present simulation, a $L \times L$ square lattice is considered. The boundary condition, used here, is periodic in both the (x and y) directions. The initial ($t = 0$) configuration, is chosen as the half of the total number (selected randomly) of spins are up ($s(x, y, t = 0) = +1$). This configuration of spins, corresponds to the high temperature disordered phase. The spins are updated randomly (a site (x, y) is chosen at random) and spin flip occurs (at temperature T) according to the Metropolis rate[23] (W)

$$W(s \rightarrow -s) = \text{Min}[\exp(-\Delta E/k_B T), 1], \quad (3)$$

where ΔE is the change in energy due to the spin flip and k_B is the Boltzmann constant. L^2 such random updates of spins constitutes the unit time step here and is called Monte Carlo Step per spin (MCSS). Here, the value of magnetic field is measured in the unit of J . And the temperature is measured in the unit of J/k_B . The dynamical steady state is reached by cooling the system slowly in small step ($\delta T = 0.02$ here) of temperature, from the high temperature, dynamically disordered configuration. This particular choice is a compromise between the computational time and the precision in measuring the transition temperature. The frequency of the propagating magnetic field wave was taken $f = 0.01$ throughout the study. The total length of the simulation is 2×10^5 MCSS and first 10^5 MCSS transient data were discarded. The data are taken by averaging over 10^5 MCSS. In some cases, near the transition points, averaging was done over 2×10^5 MCSS, after discarding initial 2×10^5 MCSS. Since the frequency of the propagating field is $f = 0.01$, the complete cycle of the field requires 100 MCSS. So, in 10^5 MCSS, 10^3 numbers of cycles of the propagating field are present. The time averaged data over the full cycle (100 MCSS) of the propagating field are further averaged over 1000 cycles.

III. Results.

In this study, a square lattice of size $L = 100$ is considered. The steady state dynamical behaviours of the spins are studied here. The amplitude, frequency and the wavelength of the propagating wave are taken $h_0 = 0.6$, $f = 0.01$ and $\lambda = 25$ respectively. The magnetic field is propagating along the y -direction (vertically upward in the graphs). The temperature of the system is taken $T = 1.50$. The configuration of the spins, at any instant of time $t = 100100$ MCS, are shown in Fig-1(a). Here, it is noted that, the clusters of spins are formed in strips and these strips move coherently as time goes on. The propagation of the spin-strips are clear in Fig-1(b), where the snapshot was taken at instant $t = 100125$ MCSS. The similar study is performed at a lower temperature $T = 1.26$ (with all other parameters of the propagating field remain same). Here, the spin clusters are observed to be formed in such shapes which are not like the strips (as observed in the case of higher temperature $T = 1.50$, mentioned above). This is shown in Fig-1(c), at any instant $t = 100100$ MCSS. These irregularly shaped spin-clusters are observed to propagate (along the direction of propagating magnetic field), which is clear from Fig-1(d) (for $t = 100125$ MCSS).

To show the propagations of these spin-clusters, the instantaneous line magnetisation $m(y, t) = (\int s(x, y, t)dx/L)$ was plotted against y at any particular instant $t = 100100$ MCSS. This is shown in Fig-2(a) (compare with Fig-1(a)). The periodic variation of $m(y, t)$ along y -direction is found. This was observed to propagate (see Fig-2(b) and compare with Fig-1(b) when shown at different time $t = 100125$ MCSS. It may be noted here, that the line magnetisation is periodic (with y) at any instant of time t . This is also periodic in time t at any position y . The oscillation is symmetric about $m(y) = 0$ line (for higher temperature $T = 1.50$). Here, the time average magnetisation over a full cycle of the propagating field is $Q = \frac{f}{L} \int \int m(y, t)dydt$, becomes zero (due to symmetric oscillation about $m(y) = 0$ line). This corresponds to a dynamically symmetric phase.

Now, for lower temperature $T = 1.26$, the spatio-temporal periodicity, of the line magnetisation, is lost. The symmetric-oscillation (about $m(y) = 0$ line) is lost here. This corresponds to a dynamically symmetry-broken phase. As a consequence, the time averaged magnetisation over a full cycle of the propagating field, becomes nonzero. These are shown in Fig-2(c) and Fig-2(d) (may be compared with fig-1(c) and fig-1(d) respectively). But the spin-clusters were observed to propagate in this case. So, as the temperature

decreases, Q becomes nonzero (lower temperature) from a zero value (higher temperature). This Q defines the order parameter of the dynamic phase transition.

The temperature variations of the dynamic order parameter Q , its variance $\langle (\delta Q)^2 \rangle$ are studied. The dynamic energy is $E = \int H(t)dt$ and the dynamic specific heat is $C = \frac{dE}{dT}$. The derivatives are calculated numerically by using the three points central difference formula[24]. All these quantities are calculated statistically over 1000 different samples. The temperature variations of Q , $\frac{dQ}{dT}$, $\langle (\delta Q)^2 \rangle$ and C are studied for two different values of the amplitude of the propagating electromagnetic field wave and are shown in Fig-3. As the temperature decreases, Q starts to grow from zero and near the transition point it becomes nonzero. Near the transition temperatures, the $\langle (\delta Q)^2 \rangle$ and C show sharp peak and $\frac{dQ}{dT}$ show a sharp dip. From the figure it is also evident that the transition occurs at lower temperature (T_d) for higher values of the field amplitude (h_0). In this case, for $\lambda = 25$, the transitions occur at $T_d = 1.88$ and $T_d = 1.29$ for $h_0 = 0.3$ and $h_0 = 0.6$ respectively. These values of the transition temperatures are obtained from the position of sharp dips of the $\frac{dQ}{dT}$ and corresponding sharp peaks of $\langle (\delta Q)^2 \rangle$ and C shown in Fig-3. Collecting all the values of the transition temperatures (T_d) (depending on the values of h_0), the comprehensive dynamical phase boundary is obtained.

This dynamic transition temperature (T_d) was observed to depend on the wave length (λ) of the propagating magnetic field wave. The temperature dependences of Q , $\frac{dQ}{dT}$, $\langle (\delta Q)^2 \rangle$ and C are studied and shown in Fig-4, for two different values of λ ($= 25$ and 50). From the figure, it is clear that, transition occurs at higher temperature (with same h_0) for higher value of the wavelength (λ). To be precise, for $h_0 = 0.3$, the transitions occur at $T_d = 1.88$ and $T_d = 1.94$ for $\lambda = 25$ and $\lambda = 50$ respectively. Here also, the values of the transition temperatures are obtained from the position of sharp dips of the $\frac{dQ}{dT}$ and corresponding sharp peaks of $\langle (\delta Q)^2 \rangle$ and C (shown in Fig-4). So, the dynamical phase boundary should shift depending on the value of λ .

In Fig-5, the dynamical phase boundaries are drawn for two different values of λ ($=25$ and 50), in the plane formed by T_d and h_0 . It is observed that the boundary shrinks inward (region of lower T and h_0) as the wavelength of the propagating magnetic field decreases.

The dynamic phase transition, mentioned above, is associated with the

divergences of relevant length scale. For this reason, the $L^2 \langle (\delta Q)^2 \rangle$ is studied as the function of temperature T . It is found that the peak of $L^2 \langle (\delta Q)^2 \rangle$ (observed at T_d) increases as L increases. This is shown in Fig-6. This result is quite conclusive to say that there exists the diverging length scale associated with the dynamic phase transition. It may be noted here, that this method was successfully employed [4] to show the diverging length scale, associated with the dynamic transition, in Ising ferromagnet driven by oscillating (but not propagating) magnetic field.

IV. Summary.

The dynamical responses of a ferromagnet to a polarised electromagnetic wave are modelled and studied here by Monte Carlo simulation in two dimensional Ising ferromagnet. In the steady state, the coherent motion (in propagating mode) of spin clusters was observed. The time average magnetisation over the full cycle of the propagating EM wave is a measure of the order parameter in the dynamic phase transition observed here. The dynamic phase transition observed here seems to be of continuous type and found to be dependent on the amplitude and the wave length of the propagating polarised EM wave. Hence, a phase boundary (transition temperature as a function of the amplitude) is drawn for two different values of the wavelengths of EM wave. The phase boundary is found to shrink (towards the lower values of the temperature and amplitude of field) for shorter wavelength.

The signature of the divergence of relevant length scale near the transition is also observed here. This observation in the case of dynamic transition is analogous to that observed in equilibrium critical phenomenon revealing the growth of critical correlation. It would be interesting to know the universality class of this dynamic phase transition. To know the universality class, one has to estimate precisely the critical exponents, through a systematic study of scaling analysis.

Acknowledgments: The library facilities provided by the University of Calcutta is gratefully acknowledged.

References

1. B. K. Chakrabarti, M. Acharyya, *Rev. Mod. Phys.*, 71 (1999) 847; See also, M. Acharyya, *Int. J. Mod. Phys. C*, 16 (2005) 1631
2. M. Acharyya and B. K. Chakrabarti, *Phys. Rev. B* 52 (1995) 6550; See also, M. Acharyya and B. K. Chakrabarti, in *Annual reviews of computational physics*, Ed. D. Stauffer, (World Scientific, Singapore), Vol.-1, (1994) 107
3. M. Acharyya, *Phys. Rev. E* 56 (1997) 2407
4. S. W. Sides, P. A. Rikvold and M. A. Novotny, , *Phys. Rev. Lett.* 81 (1998) 834
5. M. Acharyya, *Phys. Rev. E* 59 (1999) 218
6. G. Korniss, P. A. Rikvold, M. A. Novotny, *Phys. Rev. E*, 66 (2002) 056127
7. M. Acharyya, *Phys. Rev. E*, 58 (1998) 179
8. H. Park and M. Pleimling, *Phys Rev Lett* 109 (2012) 175703.
9. O. Jiang, H. N. Yang, G. C. Wang, *Phys Rev B* 52 (1995) 14911; Q. Jiang, H. N. Yang and G. C. Wang, *J. Appl. Phys.* 79 (1996) 5122.
10. Y. Au et al, *Phys. Rev. Lett.*, **110** (2013) 097201
11. A. Berger et al, *Phys. Rev. Lett* **111** (2013) 190602
12. M. Acharyya, *Int. J. Mod. Phys. C* 14 (2003) 49.
13. H. Jung, M. J. Grimson, C. K. Hall, *Phys Rev B* 67 (2003) 094411.
14. H. Jung, M. J. Grimson, C. K. Hall , *Phys Rev E* 68 (2003) 046115.
15. M. Acharyya, *Phys. Rev. E.* 69 (2004) 027105
16. M. Keskin, O. Canko, B. Deviren, *Phys. Rev. E* 74 (2006) 011110

17. U. Temizer, E. Kantar, M. Keskin, O. Canko, *J. Magn. Magn. Mater.* 320 (2008) 1787
18. M. Acharyya, *J. Magn. Magn. Mater.*, 323 (2011) 2872
19. M. Keskin, O. Canko, M. Kirak, *Phys. Stat. Solidi B*, 244 (2007) 3775;
B. Deviren, M. Keskin, *Phys. Lett. A* 374 (2010) 3119
20. M. Acharyya, *Physica Scripta*, 84 (2011) 035009
21. M. Acharyya, *J. Magn. Magn. Mater.*, 334 (2013) 11
22. M. Acharyya, *J. Magn. Magn. Mater.*, 354 (2014) 349.
23. K. Binder and D. W. Heermann, 1997, Monte Carlo Simulation in Statistical Physics (Springer Series in Solid State Sciences) (New York: Springer)
24. C. F. Gerald and P. O. Weatley, 2006, Applied Numerical Analysis (Reading, MA: Addison-Wesley); J. B. Scarborough, 1930, Numerical Mathematical Analysis (Oxford: IBH)

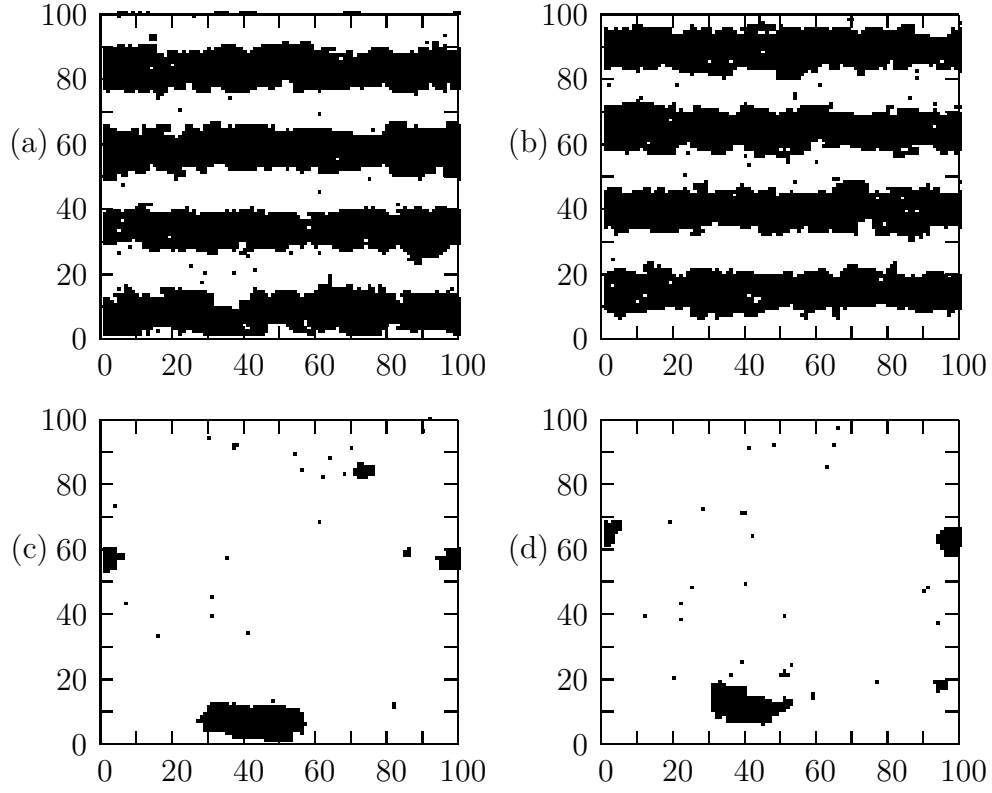


Fig-1. The motion of spin-clusters of down spins (shown by black dots), swept by propagating magnetic field wave, for different values of (a) Time = 100100 MCSS, $T=1.5$ and $h_0 = 0.6$ (b) Time = 100125 MCSS, $T = 1.5$ and $h_0 = 0.6$ (c) Time = 100100 MCSS, $T = 1.26$ and $h_0 = 0.6$ (d) Time = 100125 MCSS, $T = 1.26$ and $h_0 = 0.6$.

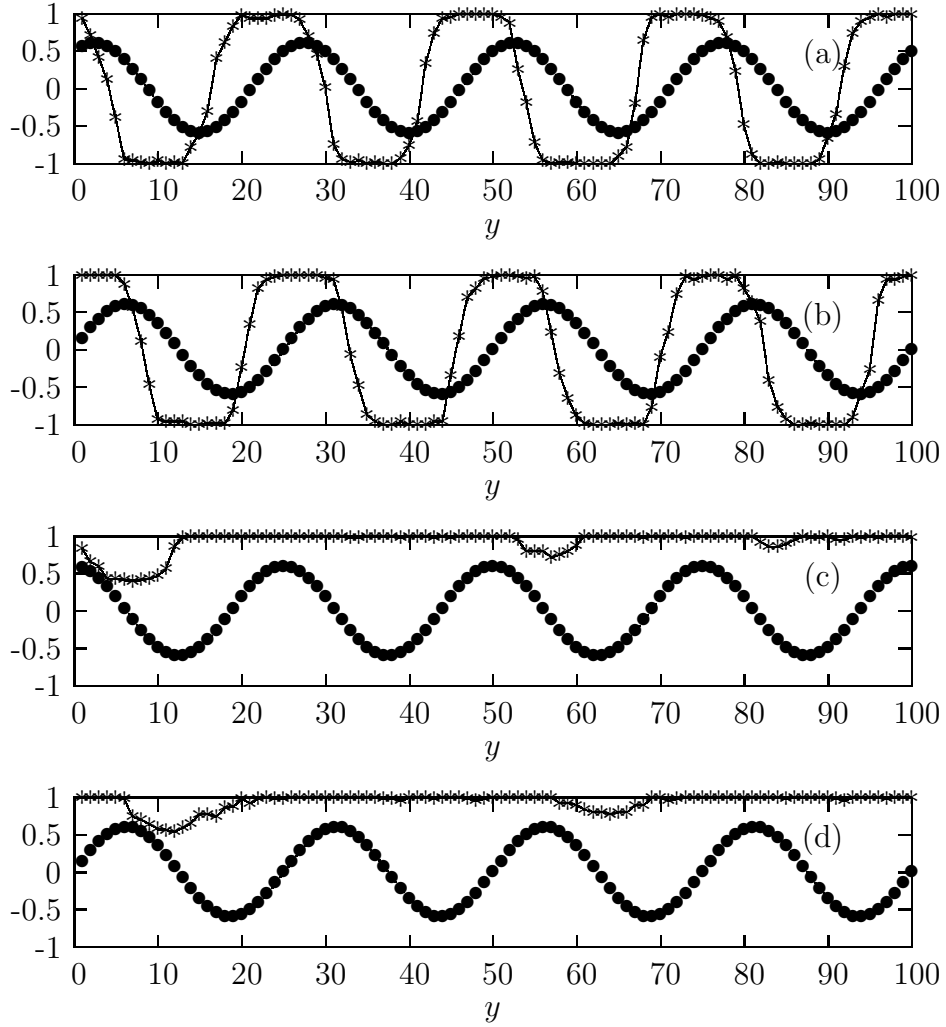


Fig-2. The propagation of field (\bullet) and the line magnetisation ($*$) for various values of (a) Time = 100100 MCSS, $T=1.5$ and $h_0 = 0.6$ (b) Time = 100125 MCSS, $T = 1.5$ and $h_0 = 0.6$ (c) Time = 100100 MCSS, $T = 1.26$ and $h_0 = 0.6$ (d) Time = 100125 MCSS, $T = 1.26$ and $h_0 = 0.6$.

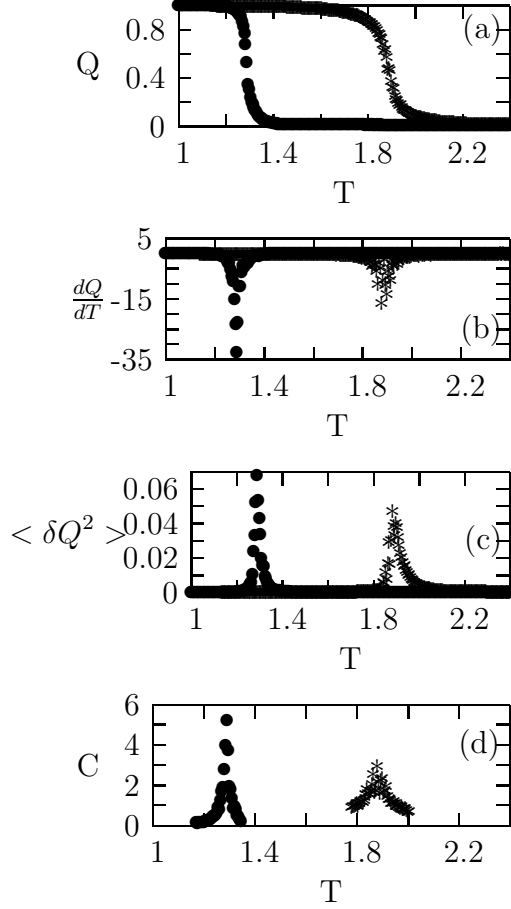


Fig-3. The temperature (T) dependences of the (a) Q , (b) $\frac{dQ}{dT}$, (c) $\langle (\delta Q)^2 \rangle$ and (d) C , for two different values of h_0 for *propagating* magnetic field wave having $f = 0.01$ and $\lambda = 25$. In each figure, $h_0 = 0.3$ (*) and $h_0 = 0.6$ (●).

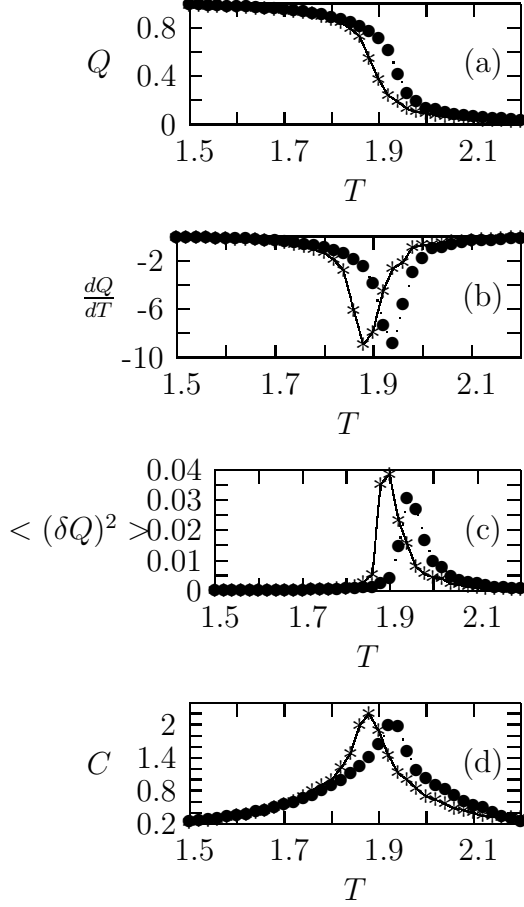


Fig-4. The temperature (T) dependences of the (a) Q , (b) $\frac{dQ}{dT}$, (c) $\langle (\delta Q)^2 \rangle$ and (d) C , for two different values of λ for *propagating* magnetic field wave having $f = 0.01$ and $h_0 = 0.3$. In each figure, $\lambda = 25$ (*) and $\lambda = 50$ (●).

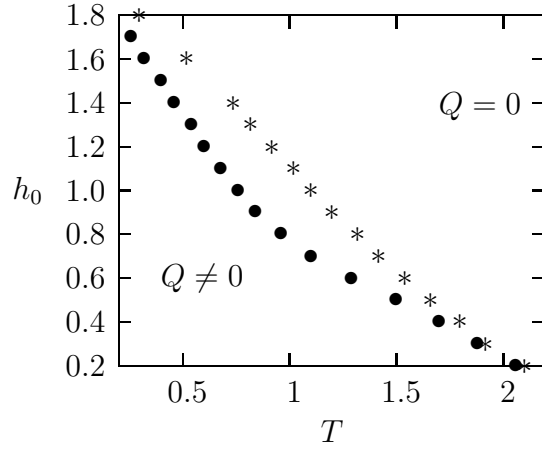


Fig-5. The phase diagram for dynamic phase transition by propagating magnetic field wave for two different values of wavelengths, $\lambda = 25(\bullet)$ and $\lambda = 50(*)$. Here, $f = 0.01$.

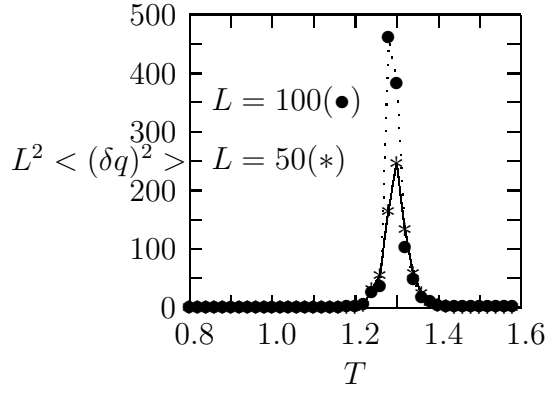


Fig-6. The plot of temperature (T) versus $L^2 \langle (\delta Q)^2 \rangle$ for different system sizes (L). Here, $h_0 = 0.6$, $\lambda = 25$ and $f = 0.01$.